

Molecular dynamics simulation of hyperthermal neutrals generated by energetic ion impact on a metal plate

Seung-hoon Park, Suk Jae Yoo, and Choong-Seock Chang

Citation: *J. Appl. Phys.* **107**, 013304 (2010); doi: 10.1063/1.3276097

View online: <http://dx.doi.org/10.1063/1.3276097>

View Table of Contents: <http://jap.aip.org/resource/1/JAPIAU/v107/i1>

Published by the [American Institute of Physics](#).

Additional information on J. Appl. Phys.

Journal Homepage: <http://jap.aip.org/>

Journal Information: http://jap.aip.org/about/about_the_journal

Top downloads: http://jap.aip.org/features/most_downloaded

Information for Authors: <http://jap.aip.org/authors>

ADVERTISEMENT



AIP Advances

Now Indexed in Thomson Reuters Databases

Explore AIP's open access journal:

- Rapid publication
- Article-level metrics
- Post-publication rating and commenting

Molecular dynamics simulation of hyperthermal neutrals generated by energetic ion impact on a metal plate

Seung-hoon Park,^{1,a)} Suk Jae Yoo,^{2,b)} and Choong-Seock Chang^{1,3}

¹Department of Physics, Korea Advanced Institute of Science and Technology, Yuseong-gu, Daejeon 305-701, Republic of Korea

²National Fusion Research Institute, Daejeon 305-333, Republic of Korea

³Courant Institute of Mathematical Sciences, New York University, Mercer Street, New York 10012, USA

(Received 30 July 2009; accepted 25 November 2009; published online 12 January 2010)

A hyperthermal neutral beam (HNB) source is one of candidate methods to reduce plasma-induced damage problems. The HNB is generated by vertical collisions between energetic ions and a reflector composed of a tungsten plate. We perform a HNB generation simulation using a molecular dynamics algorithm. The roughness of the reflector surface is experimentally measured and the surface structure is taken into consideration in the simulation. The energy and angular distributions of the HNB are obtained by the simulation and the energy yield of the reflected neutral particles is found to be in good agreement with experimental data. © 2010 American Institute of Physics. [doi:10.1063/1.3276097]

I. INTRODUCTION

Plasma processing has many applications in the area of semiconductor manufacturing.¹ However, as the feature size of semiconductor devices decreases, plasma processing has several disadvantages arising from plasma damage induced by charged particles²⁻⁴ and UV radiation.^{5,6} These disadvantages can become serious problems that decrease semiconductor yield. One of the solutions to reduce the damage by charged particles is a hyperthermal (1–100 eV) neutral beam (HNB) processing.¹⁰⁻¹²

HNB generation for material processing has been studied by a number of research groups.⁷⁻¹⁴ The most effective method of HNB generation is based on surface neutralization. Ions are neutralized through the Auger process near metal surfaces and then scattered from the surfaces, i.e., reflected. With smaller grazing angle, ions are made incident onto the metal surface and higher neutral particle and energy yields can be obtained. However, most HNB generation systems developed thus far are not suitable for commercialization due to difficulties in scale up and limitations of high flux beam extraction. In order to address these shortcomings, a new type HNB source has been developed.^{15,16}

The key issue of HNB generation is understanding ion-surface interactions and neutral transport in plasma. With low energy (≤ 100 eV) impact onto the metal surface, most ions are neutralized and scattered off, i.e., reflected, with little sputtering of surface atoms. Although the Auger or resonance process is taken for the main neutralization process,²⁰ the physics of neutral beam generation is not yet fully understood. In order to better understand the neutralization process, we have developed a molecular dynamics simulation. Molecular dynamics simulations are widely used to understand physics of ion-surface interactions considering surface condition. This method has recently been applied to

study etching, sputtering, deposition, plasma-wall interaction in Tokamak, and various research fields of ion-surface interactions.

In this paper, we report simulation results of the HNB properties as a function of the impact energy of ions onto a reflector by a molecular dynamics simulation, which has been developed for estimation of the energy and angular distributions of reflected neutrals by ion-metal surface interactions. The surface conditions are taken into account in the simulation to calculate the ion-surface interaction more accurately since the energy efficiency of neutral atoms is influenced by the surface conditions, including surface roughness, in particular. The simulation results are discussed on the basis of comparison with experimental results.

II. SIMULATION DESCRIPTION

The HNB generation system is schematically shown in Fig. 1. The ions are accelerated from the plasma sheath to the negatively biased reflector and collide with the reflector surface. The ions can be neutralized near the reflector surface through neutralization processes such as the Auger process, which is the dominant process among surface neutralization processes. As they pass through the bulk plasma, the neutral particles can be lost in the plasma by electron impact ionization, neutral-ion charge exchange, and elastic scattering with

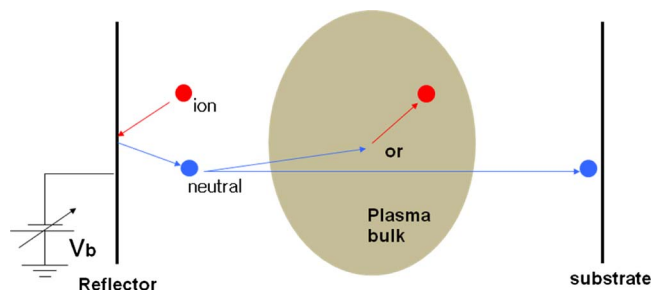


FIG. 1. (Color online) Schematic description of HNB source.

^{a)}Electronic mail: physh@kaist.ac.kr.

^{b)}Electronic mail: sjyoo@nfri.re.kr.

ions and background neutrals. We do not consider the behavior of the HNB particles in the bulk plasma but focus on reflection properties of the HNB in the simulation.

The simulation is based on a molecular dynamics algorithm. In molecular dynamics, the trajectories of atoms are solved by the Newtonian equation of motion in which atoms interact with each other. The equation is numerically integrated by the velocity-Verlet method. The particle movement is driven by the gradient of interatomic potential, $-\nabla V$. The key point of molecular dynamics is how to describe the interaction between atoms, and thus the simulation result is strongly dependent on the interatomic potentials of atoms. We use the interatomic potential between tungsten atoms obtained by the well known Finnis–Sinclair model¹⁷ modified by Ackland and Thetford,¹⁸ which describes high energy collisions well. The total potential energy is composed of two

parts. The N -body potential to express the cohesive energy as a sum over all atoms and the conventionally repulsive pair potential.

$$U_{\text{total}} = U_{\text{em}} + \frac{1}{2} \sum_{ij}^N V_p(r_{ij}), \quad (1)$$

where r_{ij} is the distance between atoms i and j ,

$$U_{\text{em}} = -A \sum_i \sqrt{\rho_i}, \quad (2)$$

and

$$\rho_i = \sum_j \phi(r_{ij}), \quad (3)$$

is the local electronic charge density at site i

$$\phi(r_{ij}) = \begin{cases} (r_{ij} - d)^2, & r_{ij} \leq d, \\ 0, & r_{ij} > d, \end{cases} \quad (4)$$

$$V_p(r_{ij}) = \begin{cases} (r_{ij} - c)^2(c_0 + c_1 r_{ij} + c_2 r_{ij}^2) + B(b_0 - r_{ij})^3 e^{-\alpha r_{ij}}, & r_{ij} \leq c, \\ 0, & r_{ij} > c. \end{cases} \quad (5)$$

The cutoff distances d and c are the second and third neighbor separations for a body-centered-cubic (bcc) metal structure, respectively. The parameters of U_{em} and V_p are empirically determined with experimental data.^{17,18}

The incident ions can be treated as energetic neutrals since most of the ions are neutralized near the metal surface.^{19,20} To simulate collisions of incident argon (Ar) atoms with the tungsten surface, the screened Coulomb potential is used, such as in the Moliere type potential formula, which is a purely repulsive potential since the Ar atoms have low reaction with the other species atoms.

$$V(r_{ij}) = \frac{Z_i Z_j e^2}{4\pi\epsilon_0 r_{ij}} \{0.35e^{-0.3r_{ij}/a} + 0.55e^{-1.2r_{ij}/a} + 0.10e^{-6.0r_{ij}/a}\}, \quad (6)$$

where

$$a = 0.8 \frac{0.8854a_0}{(Z_i^{0.5} + Z_j^{0.5})^{2/3}}, \quad (7)$$

Z_i and Z_j are the nuclei charges, and a is the screening length, which is 0.8 times the Firsov length. The screening length a describes the length screened by electron clouds surrounding ions and a_0 is the Bohr radius. This potential is applied at short range and there exists a cutoff length, the value of which is determined by two times the lattice constant of the bcc tungsten.

In order to mimic an actual rough reflector, the surface roughness should be considered in the simulation. Due to the computational difficulty in the simulation of a large-scaled

rough surface of several centimeters, the incident angles of ions with respect to the rough surface are defined in multi-scale. Initially, the ions are assumed to be incident parallel to the normal of the large-scaled surface, which is assumed to be ideally flat in spite of the rough surface structure. The incident angles are then defined as the angles between the slopes of the rough surface structure and the normal of the large-scaled surface [see Fig. 2(b)].

The rough surface structure of a tungsten reflector is described with surface roughness measured experimentally. For the molecular dynamics simulation, with the incident angles determined by slopes of the rough surface structure, in an atomic scale, ions collide with the lattice structure of the tungsten surface.

For the atomic scale simulation, as shown in Fig. 3, a tungsten (0 0 1) surface is prepared with cell dimensions (x, y, z) of $31.65 \times 31.65 \times 22.16 \text{ \AA}^3$. A tungsten atom number of 1400 is included in a cell. The periodic boundary condition along the x - y plane is applied to the simulation cell to remove the finite size effect. A free boundary condition is set along a half direction of the z -axis and in the other half direction two layers at the bottom are fixed so as to prevent drifting of surface atoms. For all ion impact events, non-physical heat arises in the simulation cell. Thus, in order to control temperature during bombardments, a Berendsen thermostat²¹ is applied to $\sim 6 \text{ \AA}$ above the bottom layer during all impact events. The control temperature is 300 K. In order to evolve a local rough surface configuration by ion impacts, the local rough surface is prepared by melt-quench

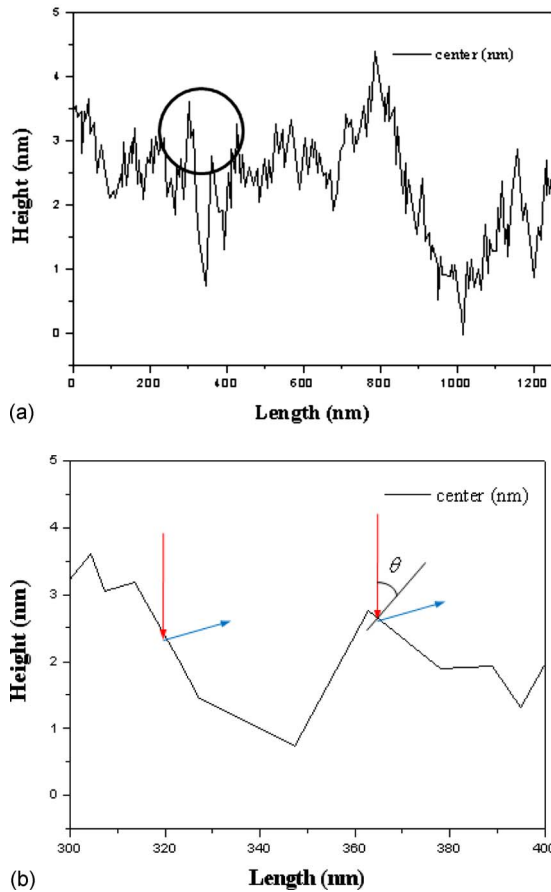


FIG. 2. (Color online) (a) Local surface measured experimentally at the center of the reflector. The roughness is 2.37 nm. (b) Enlarged surface is a part of (a) [black circle in (a)]. The incident angle determined by the slope of the surface.

procedure in atomic scale before the impact simulation. The surface is somewhat rough as a result of the melt-quench procedure.

We assume that ions should be vertically incident on the large scale surface and randomly impact it. In an atomic scale, the initial ion location is set at a z-position out of the interaction range with the surface atoms. The ions bombard the bcc tungsten surface with incident angles that are determined by slopes of the large scale surfaces. Each impact

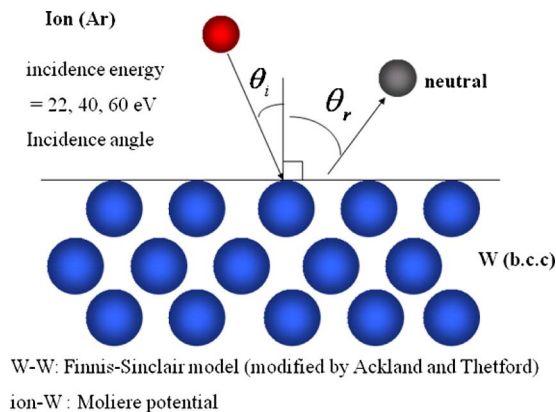


FIG. 3. (Color online) System description of bcc tungsten (0 0 1) surface for molecular dynamics.

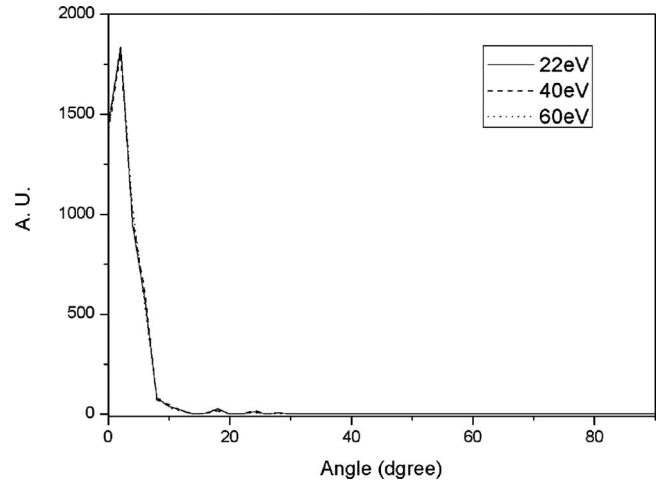


FIG. 4. Incident ion angular distribution determined by the slopes of the rough surface.

simulation is performed during 1 ps with a time step of 0.5 fs. At the end of the impact, the angle and energy of the reflected neutrals are recorded.

III. RESULTS AND DISCUSSION

The rough surface structure measured experimentally at the center of the reflector is shown in Fig. 2(a). To depict the determining incident angle of ions, the enlarged experimental rough surface of a reflector is described in Fig. 2(b). When ions are normally incident onto the large-scaled surface, ions feel the slope of rough surface structures. The incident angle of ions at a rough surface point is shown in Fig. 3 for the molecular dynamics simulation. The roughness is 2.37 nm, as determined by mechanical definition, $Ra = \sum_i^N |h_i| / N$, where h_i is the height of a rough surface structure.

The incident angles for the atomic scale simulation determined by the angles between the slopes of rough surface structures and the trajectory of ions normally incident on the large-scaled surface are shown in Fig. 4. Most of the incident ions are initially distributed at an incident angle smaller than 10° .

The energy distribution of neutral particles reflected at the neutralizer surface is shown in Fig. 5. Ions with an en-

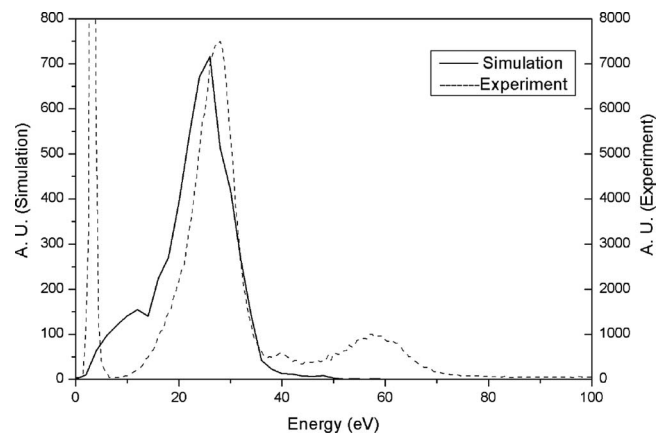


FIG. 5. Energy distribution of neutrals at 60 eV incidence energy. Comparison with experimental results (Ref. 15) at bias -60 V.

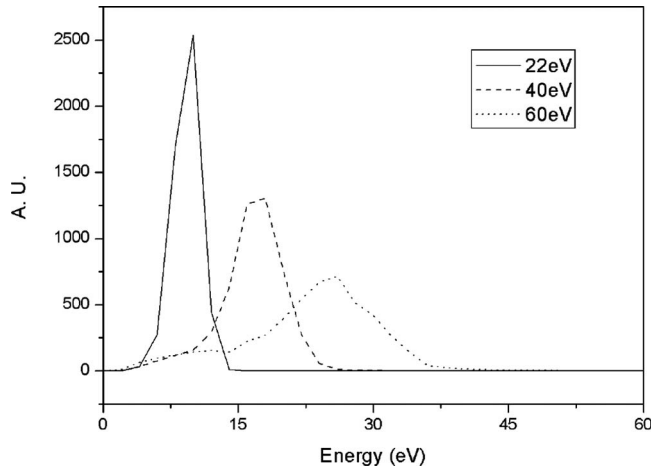


FIG. 6. Energy distribution of reflected neutral atoms with 22, 40, and 60 eV incident energy.

ergy of 60 eV are vertically incident onto the reflector. The impact of ions onto the reflector plate is simulated in order to investigate the distributions of reflected neutrals. The energy of reflected particles can be simply explained by the binary collision approximation in the case where the incident ions collide with lattice atoms of tungsten at the reflector surfaces and the energy ratio is shown in²²

$$\frac{E_r}{E_i} = \left(\frac{1}{\mu^{-1} + 1} \right)^2 (\cos \chi \pm \sqrt{\mu^{-2} - \sin^2 \chi})^2, \quad (8)$$

where E_r and E_i are the reflected and incident energies, χ is the scattering angle, and $\mu = M_i/M_t$ is the mass ratio of incident and target atoms. For a direct, head-on-collision, $\chi = \pi$, the energy ratio, E_r/E_i , is ~ 0.4 . The energy ratio a tungsten surface is approximately 0.4 in Fig. 5. The energy distribution obtained by simulation was compared with experimental data. In the experimental result, the first peak is the energy distribution of the background plasma ions of which the energy corresponds to the plasma potential. Compared with experimental data, the energy distribution of the second peak is in good agreement with the simulation results.¹⁵ There is a discrepancy of between experimental results and simulation data. The monoenergetic ions are only considered in this simulation whereas the other energy groups of ions can exist in the bulk plasma. The discrepancy can also be explained with consideration of total reflector surface structure. Although the surface in simulation cell used rough surface structure in order to mimic the real situation, the various lattice structures in the real situation are mixed in the reflector surface whereas (001) orientation is used in the simulation. In the bulk plasma, doubly charged (i.e., Ar^{2+}) ions can exist ($\sim 10\%$).²³ The energy of Ar^{2+} ions accelerated by reflector bias is twice as high as energy of Ar^+ . The doubly charged ions could cause the third energy peak in the experimental data.

In order to obtain a low energy neutral beam, ions with an energy lower than 60 eV should be employed. Figure 6 shows the energy distribution as a function of the incident ion energy. The energy of neutrals decreases as the incident ion energy is decreased. The energy ratio of neutral to ion

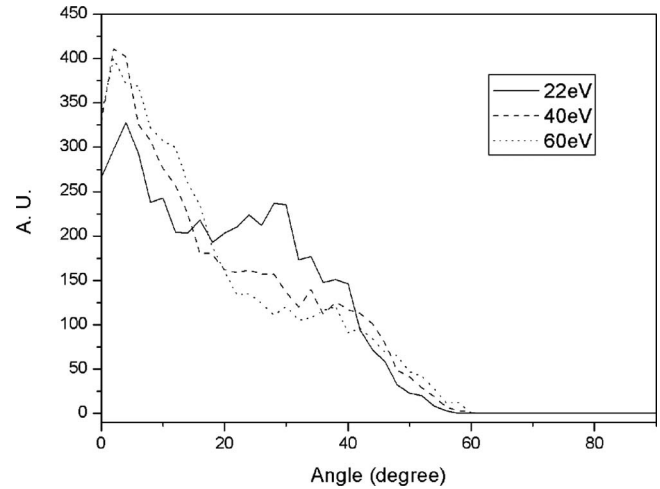


FIG. 7. Angular distribution of reflected neutral atoms with 22, 40, and 60 eV incident energy.

energies is about 0.4–0.5. This agrees well with the binary collision model but the energy distributions are slightly different from each other. When surface atoms are locally heated by energetic ions and vibrate, the motions of surface atoms thereupon influence reflected neutrals in the same time scale. The time scale of the collision between incident ions and surface atoms is in the same time scale of collision cascade between surface atoms. The incident ions collide with more surface atoms as the energy of incident ions increase. Therefore, as the incident energy increases, the vibration of surface atoms increase and then the motion of reflected neutrals are influenced strongly by the surface atoms. As a result, the energy distribution of reflected neutrals becomes broader.

The angular distribution of neutral particles is difficult to measure experimentally and thus is instead inferred from the simulation results. Figure 7 shows an angular distribution of reflected particles. The angular distribution can be broadened by the lattice structure and surface roughness of the reflectors. The broadening of the angular distribution is caused mainly by the surface roughness for angles smaller than 20° and mainly by the lattice structure for angles larger than 20° .

The slopes of the rough surface structure are angularly distributed within 10° , as shown in Fig. 2, and thus the incident angles of ions should be distributed within 10° , as shown in Fig. 4. If the surface roughness is taken into account in the binary collision approximation, in which specular scattering is assumed, the angles of the reflected neutral particles should be distributed within 20° . However, at an atomic scale, the reflector surface is not perfectly specular due to the lattice structure. The incident ions, which are out of head-on collisions with the lattice atoms of the reflector are reflected with a wider angle than those of head-on collisions which is assumed in the binary collision approximation. Thus, the angular distribution broader than 20° can be explained by the lattice structure of the reflector.

IV. CONCLUSION

A molecular dynamics simulation was developed to investigate the characteristics of HNBS generated by ion-

surface interaction. Ions are vertically incident onto a tungsten reflector and then neutralized and scattered-off as neutral particles, i.e., reflected. In order to take into consideration the actual experimental conditions, the surface roughness measured experimentally is taken into account in the simulation. The energy distribution of the neutral beam is in good agreement with experimental results. The energy ratio of the neutral beam is 0.4–0.5 for each incident ion energy in the case of normal incidence onto the reflector. The results can be explained by using the binary collision approximation model. The angular distribution of smaller angles is thought to be caused mainly by the surface roughness and that of larger angles mainly by the lattice structure. In future research, we plan to study the transport of reflected neutral particles in bulk plasmas to investigate neutral flux onto substrates.

ACKNOWLEDGMENTS

This work was supported by Development Program of Nano Process Equipments of Korea Ministry of Knowledge Economy and the Korean BK21 Program.

¹M. A. Lieberman and A. J. Lichtenberg, *Principles of Plasma Discharges and Materials Processing* (Wiley, New York, 1994).

²G. S. Hwang and P. Giapis, *J. Vac. Sci. Technol. B* **15**, 70 (1997).

³A. D. Bailly III and R. A. Gattocho, *Jpn. J. Appl. Phys., Part 1* **34**, 2083 (1995).

⁴K. Hashimoto, *Jpn. J. Appl. Phys., Part 1* **33**, 6013 (1994).

⁵X. Tang, Q. Wang, and D. M. Manos, *J. Vac. Sci. Technol. B* **18**, 1262 (2000).

⁶T. Okamoto, T. Ide, A. Sasaki, K. Azuma, and Y. Nakata, *Jpn. J. Appl. Phys., Part 1* **43**, 8002 (2004).

⁷K. P. Giapis, T. A. Moore, and T. K. Minton, *J. Vac. Sci. Technol. A* **13**, 959 (1995).

⁸T. Yunogami, K. Yokogawa, and T. Mitzutani, *J. Vac. Sci. Technol. A* **13**, 952 (1995).

⁹M. J. Goeckner, T. K. Bennett, and S. A. Cohen, *Appl. Phys. Lett.* **71**, 980 (1997).

¹⁰D. J. Economou, *J. Phys. D: Appl. Phys.* **41**, 024001 (2008).

¹¹S. Samukawa, *Jpn. J. Appl. Phys., Part 1* **45**, 2395 (2006).

¹²B. J. Park, S. W. Kim, S. K. Kang, K. S. Min, S. D. Park, S. J. Kyung, H. C. Lee, J. W. Bae, J. T. Lim, D. H. Lee, and G. Y. Yeom, *J. Phys. D* **41**, 024005 (2008).

¹³S. J. Kim, S. J. Wang, J. K. Lee, D. H. Lee, and G. Y. Yeom, *J. Vac. Sci. Technol. A* **22**, 1948 (2004).

¹⁴D. J. Economou, *Plasma Processes Polym* **6**, 308 (2009).

¹⁵Mi. Joung, M. Cho, W. Namkung, S. J. Yoo, T. Lho, M. Bok, and D. Kim, *J. Korean Phys. Soc.* **53**, 3749 (2008).

¹⁶S. J. Yoo, D. C. Kim, M. Joung, J. S. Kim, B. J. Lee, K. S. Oh, K. U. Kim, Y. H. Kim, Y. W. Kim, S. W. Choi, H. J. Son, Y. C. Park, J.-N. Jang, and M. P. Hong, *Rev. Sci. Instrum.* **79**, 02C301 (2008).

¹⁷M. W. Finnis and J. E. Sinclair, *Philos. Mag. A* **50**, 45 (1984).

¹⁸G. J. Ackland and R. Thetford, *Philos. Mag. A* **56**, 15 (1987).

¹⁹B. A. Helmer and D. B. Graves, *J. Vac. Sci. Technol. A* **16**, 3502 (1998).

²⁰H. D. Hagstrum, *Phys. Rev.* **96**, 336 (1954).

²¹H. J. C. Berendsen, J. P. Postma, W. F. van Gunsteren, A. DiNola, and J. R. Haak, *J. Chem. Phys.* **81**, 3684 (1984).

²²P. G. Bertrand and J. W. Rabalais, in *Low Energy Ion-Surface Interactions*, edited by J. W. Rabalais (Wiley, New York, 1994).

²³A. Bogaerts and R. Gijbels, *J. Appl. Phys.* **86**, 4124 (1999).